Journal of Inorganic and General Chemistry
ZAAC
Zeitschrift für anorganische und allgemeine Chemie
DOI: 10.1002/zaac.202000098
ARTICLE

Effect of Oxygen on High-temperature Phase Equilibria in Ternary Ti-Al-Nb Alloys

Benedikt Distl,*[a] Gerhard Dehm,[a] and Frank Stein[a]

Dedicated to Professor Juri Grin on the Occasion of his 65th Birthday

Abstract. Alloys based on titanium aluminides received a lot of attention because of their capability to substitute Ni-based superalloys in high-temperature applications. However, the phase equilibria between the main microstructure constituents (αTi), (βTi), γ (TiAl) and α_2 (Ti_3Al) can be shifted significantly by impurities such as oxygen especially at high temperatures. This behavior is investigated on the tie-triangle (αTi) + (βTi) + γ (TiAl) in the ternary Ti-Al-Nb system at 1300 °C. An explanation for this behavior could be the occupation of octahedral voids by impurities in certain phases.

Introduction

Light-weight alloys based on intermetallic phases of the Ti–Al system (Figure 1)[1] are in the research focus in the last decades due to their capability to substitute Ni-based superalloys in certain high-temperature, high-strength applications such as jet engine turbine blades[2] or turbo charger rotors.[3] Alloys for such applications are mainly based on a combination of the two intermetallic phases (γ (TiAl) ($L1_0$, *tP*4, *P*4/*mmm*) and α_2 (Ti_3Al) ($D0_{19}$, *hP*8, $P6_3/mmc$). In this composition range a large variety of microstructures can be designed by addition of alloying elements to adjust the mechanical properties. A strong focus lies on the development of alloys, where by addition of elements such Nb, Mo or W the cubic (βTi) (A2, *cI*2, $Im\bar{3}m$) phase is stabilized at high temperatures allowing hot working of the otherwise very brittle material.

The design of such alloys is currently done mainly by costly trial and error experiments. It would be much more time- and cost-effective to use computational approaches such as the CALPHAD method,[4] which is well suited to calculate and predict all relevant thermodynamic data for alloy development. However, such methods need accurate data which are not available for the system Ti-Al-Nb. The inappropriateness of databases is often related to one or more of the following problems: (i) the number of systematic phase equilibria studies over the entire composition range of a system is very limited or even zero; (ii) there are already differences in underlying binary systems; (iii) reported datasets are often contradicting to each other; (iv) phase relations and phase transformation mechanisms are not fully understood;[5,6] and (v) most studies neglect the influence of impurity elements (O,[7,8] N, C[9]) on the phase stability and phase compositions.

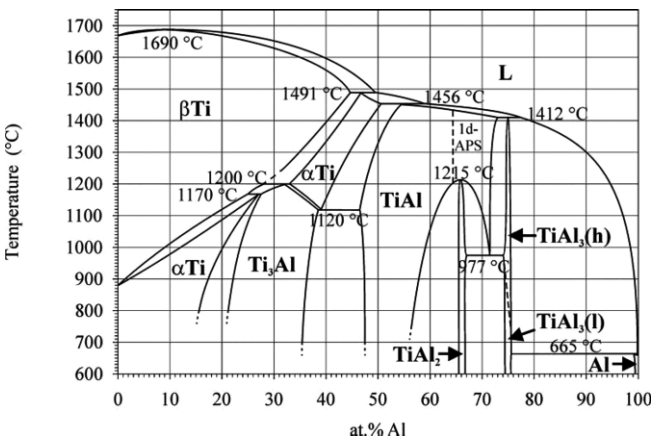

Figure 1. Binary Ti–Al phase diagram[1].

Since oxygen is inherent to Ti, it is important to consider especially the effects of oxygen on the phase equilibria. It is known that in the binary Ti-Al system, the phase boundaries between (αTi)/(βTi) and (αTi)/α_2 (Ti_3Al) shift significantly to lower Al content with increasing amounts of oxygen.[7] A similar behavior can be observed in ternary Ti-Al-X systems where equilibrium phase compositions of three-phase equilibria involving the (αTi) or α_2 (Ti_3Al) phase change to higher amounts of the third element as a result of increased impurity contents in the alloy.[8,9] As the solubility of impurities especially in (αTi)/α_2 (Ti_3Al) is very high,[10–12] exceeding by far the impurity levels even of industrial alloys,[13] no oxides, carbides or nitrides form in the bulk. This means that from inspecting the microstructure there are no indications for the presence and amount of oxygen.

Therefore, the available phase equilibria data need to be treated very carefully since in the past the amount of impurities was either not measured or only checked after alloy synthesis

* B. Distl
E-Mail: distl@mpie.de
[a] Max Planck Institut für Eisenforschung GmbH
Max-Planck-Str. 1
40237 Düsseldorf Germany

(i.e. not after heat treatment). Even in cases where a high contamination of the material was mentioned, a possible influence on phase equilibria was ignored.[14] Moreover, as Ti, and thereby Ti-Al based alloys, are prone to oxygen, it is very likely that the alloys take up additional oxygen not only during synthesis, but also while being heat-treated making it important to check impurity contents afterwards. Not considering the presence of impurities can lead to complete misidentification of phases as was pointed out by *Schuster*[15] for example in the Al-Nb system.

All these challenges are considered in the scope of the currently running European project ADVANCE,[16] where the authors are one of the project partners performing detailed studies on phase equilibria in a temperature range of 700–1300 °C for different Ti-Al-X systems to improve an existing CALPHAD database for Ti-Al based alloy systems. The present article deals with the observation that, even though no oxides are formed, the presence of oxygen seems to have a significant effect on high-temperature phase equilibria in ternary Ti-Al-Nb alloys. In the following, own experimental results for phase equilibria at 1300 °C are compared with available data from literature. The reason for choosing this temperature is threefold: (i) 1300 °C is the upper limit of heat treatment temperatures in the project, and as the uptake of oxygen increases with increasing temperature and we expect the strongest effect on phase equilibria at this temperature. (ii) According to existing literature and our own preliminary results, the phase relations at 1300 °C are simpler than at lower temperatures since all solid-state reactions are finished. (iii) Finally, some literature about experimental work on phase equilibria at this temperature is available where information about impurity contents of the respective alloys is included.[17–19] After presenting the results and comparing them with literature, an attempt to explain the observed behavior is discussed. In the end, own experimental efforts to keep the oxygen levels as low as possible during alloy synthesis and heat treatments are described in the Experimental section.

Results

The alloys shown in Table 1 were heat-treated and analyzed as described in the Experimental section. Alloys N1 and N2 show a lamellar two-phase microstructure consisting of γ (TiAl) and (αTi). Alloy N4 contains the three phases (αTi) + (βTi) + γ (TiAl) (Figure 2). The big bright (βTi) grains have undergone a partial decomposition (Figure 2) and some needle-like (αTi) phase has precipitated. Alloy N3, N5 and N6 are almost exclusively (βTi) with small amounts of an additional phase being present at the grain boundaries. As mentioned, oxygen uptake during heat treatment must be checked very carefully since oxygen impurities can shift the phase equilibria compositions significantly. As shown in Table 2, the increase in oxygen content during heat treatment could be kept successfully on a very low level.

Table 1. Compositions of the alloys in as-cast condition measured with ICP-OES.

Sample no.	Ti /at.%	Al /at.%	Nb /at.%
N1	51.7	43.4	4.9
N2	48.3	45.8	5.9
N3	50.4	39.6	10
N4	43	44.7	12.3
N5	52.8	37.2	10
N6	50.3	32.4	17.3

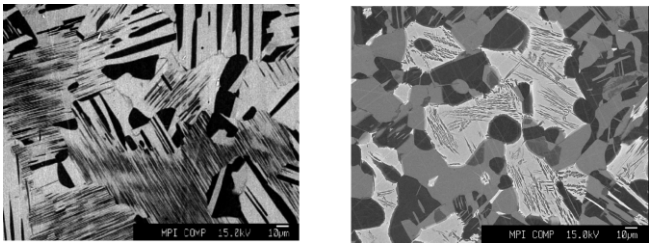

Figure 2. Microstructure of alloy N2(left) and alloy N4 (right) after water quenching from 1300°C.

Table 2. Comparison of oxygen content measured with inert gas fusion of alloys N1–N6 between as-cast and heat-treated sample at 1300 °C for 20 h.

Alloy	As cast /wt ppm	Heat-treated /wt ppm
N1	150	220
N2	140	150
N3	290	300
N4	200	Not measured
N5	190	Not measured
N6	160	280

At 1300 °C most investigations on phase equilibria in literature[17–19] are done with alloys ranging from 40–50 at.% Al focusing on the tie-triangle (αTi) + (βTi) + γ (TiAl) since this is the relevant composition range for industrial applications. In Figure 3 this tie-triangle obtained by *Kainuma* et al.[17] (ca. 240 wt ppm O in as cast alloys), *Nakamura* et al.[18] (ca. 350 wt ppm O in as cast alloys), *Xu* et al.[19] (ca. 400 wt ppm O in as cast alloys), and the present work (ca. 200 wt ppm O in as cast alloys) is plotted. As can be seen, the phase compositions vary significantly between the different studies (Table 3). All samples from literature studies were prepared either by arc- or plasma-arc-melting with several re-melting steps to achieve homogeneity. Due to the use of different raw materials, the oxygen content in the as-cast samples varies between 200–400 wt ppm. In addition, *Xu* et al.[19] homogenized their samples in fused silica ampoules backfilled with Ti-gettered argon for 5h at 1400 °C followed by furnace cooling to 1300 °C and holding there for 20–110 h. After heat treatment, they removed 1 mm from the sample surface to minimize the influence of the reaction layer between sample and fused silica formed during the heat treatment. However, fused silica is known to be no longer gas-tight at such temperatures and can start to soften and collapse already above 1100 °C.[20,21] Therefore, it is very doubtful how effective the removal of the surface layer is since our own investigations on cylindrical samples (Ø16 × 10 mm) reveal that alloys heat-treated at 1100 °C for 200 h already contain significantly higher amounts of oxygen (ca. 500 wt ppm) than alloys after 400 h at 1000 °C (ca.

220 wt ppm). The chemical analyses were performed with parts of the sample taken from near the center of the alloys indicating that oxygen diffuses through the entire cross section of the samples at these temperatures. Since the samples of *Xu* et al.[19] with dimensions of $8 \times 8 \times 9$ mm^3 are smaller in size and the heat treatment temperature is 1300 °C, it can be assumed that the oxygen content in the heat-treated sample is significantly higher as in the as-cast state.

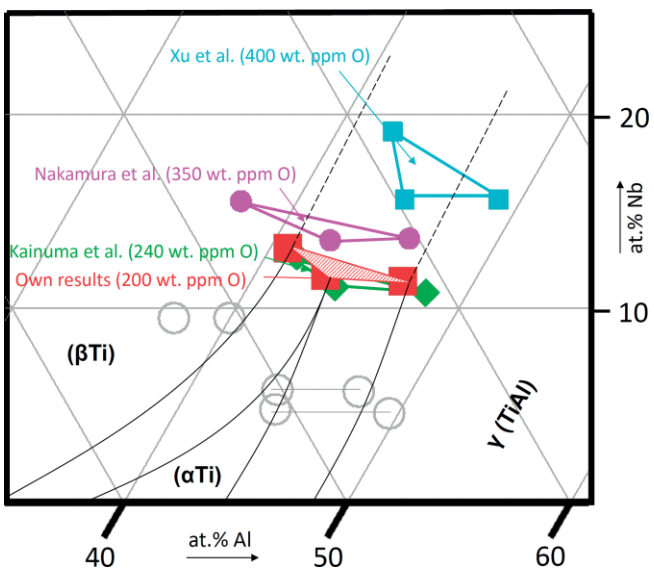

Figure 3. Partial isothermal section of Ti–Al–Nb at 1300°C with experimental results from Kainuma et al.[17], Nakamura et al.[18] Xu et al.[19] and own results regarding the tie-triangle (αTi)+(βTi)+γ (TiAl) (filled symbols) with experimentally determined phase boundaries (solid lines) and extrapolated phase boundaries (dashed lines).

Table 3. Comparison between the oxygen content in as-cast alloys and the Nb-content in the (αTi) phase of *Kainuma* et al.,[17] *Nakamura* et al.,[18] *Xu* et al.[19] and experimental results of this work after heat treatment at 1300 °C for 20 h.

Study	Oxygen content in as-cast alloy /wt ppm	Nb-content /at % in the (αTi) phase
Kainuma et al. [17]	240	11.1
Nakamura et al. [18]	ca. 350	12.5
Xu et al.[19]	ca. 400	16.0
This work	ca. 200	11.7

To minimize the effects of impurity uptake, *Kainuma* et al.[17] wrapped their samples in Mo foil. Moreover, their heat treatment time of 24 h is short compared to the 110 h of *Xu* et al.[19] In the study of *Nakamura* et al.,[18] the heat treatment was performed for 48 h at 1300 °C with samples encapsulated in fused silica ampoules. Unfortunately, none of the authors measured the impurity contents after heat treatment. Therefore, the oxygen content of the as-cast alloys is used here for comparison of the results. From the experimental results (Figure 3) it is evident that as-cast samples with low impurity contents (*Kainuma* et al.[17] and present work) result in phase compositions with the lowest Nb contents after heat treatment. The results from *Nakamura* et al.[18] and *Xu* et al.[19] are shifted to higher Nb contents. This increase of Nb solubility in the (αTi)-phase with increasing oxygen content leads to some questions. Do phases of the displayed tie-triangle differ with respect to the effect of oxygen on Nb solubility? Is only the (αTi)-phase affected by oxygen? How can the relation between oxygen content and Nb solubility be explained?

Discussion

The formation of oxides during high-temperature treatment of TiAl-based alloys is well investigated,[22,23] as well as the influence of alloying elements on this process.[22,24] Oxide scales only form on the surface of alloys and there are no reports of oxide formation within the bulk of the alloy, unless the phases present are saturated with oxygen.[11] The Ti-Al-O phase diagram shows that the solubility of oxygen in γ (TiAl) is very low compared to α_2 (Ti_3Al) and (αTi).[12] This is in good agreement with atom probe tomography measurements from *Menand* et al.[11] who concluded that oxygen in a γ (TiAl) + α_2 (Ti_3Al) two-phase microstructure almost exclusively occupies octahedral voids in α_2 (Ti_3Al). In addition, these investigations show that oxygen solubility in γ (TiAl) varies slightly with Ti concentration but does not exceed 500 at ppm,[11] which is in agreement with the phase diagram.[12]

There are two types of unoccupied octahedral voids in the α_2 (Ti_3Al) structure: (i) formed by 4 Ti atoms and 2 Al atoms (Ti_4Al_2), and (ii) formed by 6 Ti atoms (Ti_6). Neutron diffraction measurements from *Jones* et al.[25] indicate that oxygen atoms in α_2 (Ti_3Al) only occupy Ti_6 octahedral voids, what was also indicated by APT-measurements of *Menand* et al.[11] Since this kind of octahedral void exist,[11] this could be an explanation for the low solubility of oxygen since the size of the octahedral voids in both phases is similar.[11] A possible explanation for preferred occupation of Ti_6 octahedral voids by oxygen in α_2 (Ti_3Al) is the "chemical environment" of these voids. DFT calculations of *Bakulin* et al.[26] show that the absorption energy of oxygen is substantially decreased (by 1.47 eV) if aluminum is present in nearest neighbor locations of the oxygen, what is the case in Ti_4Al_2 octahedral voids. Since higher absorption energy means stronger bonds between oxygen and matrix atom, this indicates that Ti_6 octahedral voids are energetically more favorable.[26]

These results are in agreement with *Wei* et al.[27] who calculated the formation energy of octahedral and tetrahedral voids in γ (TiAl) and α_2 (Ti_3Al) occupied by oxygen. The negative values of the formation energy indicate that occupied voids are more stable than unoccupied ones. Also, Ti_6 octahedral voids in α_2 (Ti_3Al) exhibit the lowest formation energy, indicating that oxygen energetically favors the occupation of this type of voids,[27] which is in agreement with experimental findings of *Menand* et al.[11] and *Jones* et al.[25] From electronic structure calculations using the so-called "empirical electron theory of solids and molecules" method, *Zhi* et al.[28] concluded that impurities such as oxygen change hybridization states of Ti which leads to a considerably anisotropic electronic structure.

This is in agreement with *Bakulin* et al.,[26] who explained the decrease in absorption energy if aluminum is present with

a decrease in charge transfer from Ti atoms to oxygen while charge transfer between Al atoms and oxygen is high. This results in a minimal charge transfer in Ti_6 octahedral voids which is caused by stronger localization of s-, d-states of Ti atoms compared to more delocalized s-, p-states of Al.[26] This leads to an increase of covalent electrons in the bond between impurity element and metal atom and a decrease in bond strength between Ti and Al atoms.[28] All these facts point to the conclusion that oxygen prefers the more stable Ti_6 octahedral voids and therefore solubility of oxygen is higher in phases such as α_2 (Ti_3Al) that provide this kind of voids.

In addition to the change in electronic structure, the lattice parameter along the [11–20] and [0001] axis of the elementary cell increases linearly with oxygen content. Along the [11–20] axis, this change is one order of magnitude smaller than along the [0001] axis as *Jones* et al.[25] concluded from their neutron diffraction experiments on different single phase α_2 (Ti_3Al) alloys with different oxygen contents and constant Ti/Al ratio. The same behavior has been observed by *Dechamps* et al.[29] in (αTi) and the degree of lattice expansions in both phases are in agreement.[25] *Jones* et al.[25] explain the more pronounced increase along the [0001] axis of the crystal structure by the fact that in α_2 (Ti_3Al) the octahedra share one face with each other and form rows along the [0001] direction (Figure 4).[25] The increase of lattice parameters results in bond lengthening of Ti–Al and Ti–Ti bonds along the [0001] axis as a function

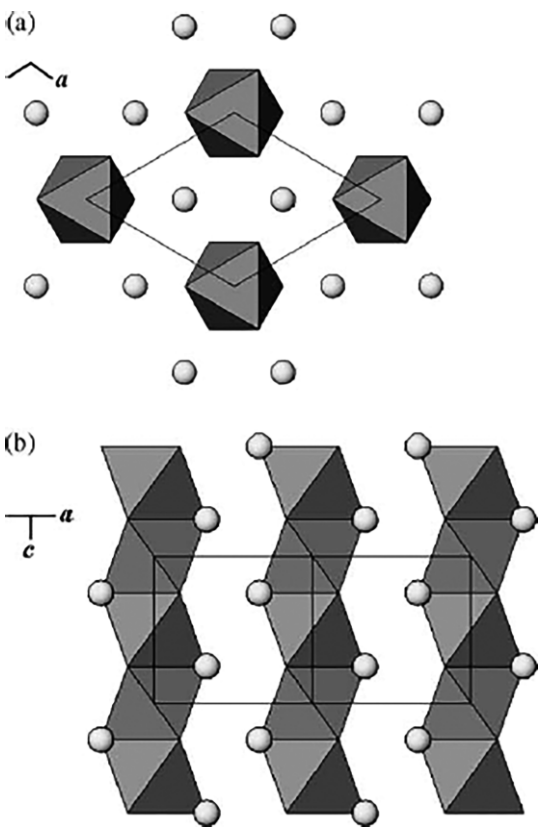

Figure 4. Crystal structure of . α_2 (Ti_3Al(O)) viewed along two directions: a, [0001]; b, [11-20]. The spheres represent Al atoms and the octahedra represent [OM6] groups (M = Ti or Al)[26].

of the oxygen content leading to a distortion of octahedral voids.[25] This leads to the question how does this distortion of the crystal structure/octahedral voids influence the solubility of Nb in (αTi) at 1300 °C?

From Figure 3 one can see that with increasing oxygen content in the as-cast alloys, the position of the (αTi) + (βTi) + γ (TiAl) tie-triangle shifts approximately parallel to the Ti-Nb axis to higher Nb contents. This means that the solubility of Nb in (αTi) increases and a higher fraction of Ti atoms can be replaced by Nb atoms due to the presence of oxygen. This agrees with DFT calculations of *Holec* et al.,[30] who showed that Nb preferentially occupies the Ti site in α_2 (Ti_3Al). Hence, some Ti_6 octahedral voids must become $Ti_{6-x}Nb_x$ voids, which appear to be a favorable configuration of these voids. The addition of a third element into the crystal structure has two effects: (i) the different size of the atom leads to a further distortion in the crystal structure/voids, and (ii) the electronic structure changes. The calculations of *Holec* et al.[30] show that the main contribution of a third element is attributed to the change in electronic structure, while the different size of the atom has only a minor effect. This means that oxygen incorporated in Ti_6 octahedral voids most likely enhances Nb uptake in the (αTi) phase. However, this effect is still far from completely understood. Some open questions are: (i) How many Ti atoms are replaced by Nb atoms in the Ti_6 octahedra; (ii) Since there are no superlattice reflections in XRD measurements it has to be assumed that the Nb atoms occupy the Ti sites randomly. This might lead to a variety of different $Ti_{6-x}Nb_x$ octahedral voids, and (iii) How do Nb atoms change the electronic structure in octahedral voids?

Conclusions

By reviewing literature about phase equilibria in the ternary Ti-Al-Nb system at 1300 °C and comparing them to own results, it could be shown that the amount of oxygen in heat-treated alloys can have a significant impact on phase equilibria at high temperatures. This proves the necessity to carefully control the oxygen level in Ti-Al alloys and try to keep impurity levels as low as possible.

As pointed out, oxygen atoms occupy Ti_6 octahedral voids which leads to a distortion of the crystal structure as function of oxygen content. The incorporation of Nb changes the electronic structure in the crystal and since Nb substitutes with Ti, $Ti_{6-x}Nb_x$ octahedral voids might be formed. However, the exact mechanism that could explain how Nb atoms influence the electronic structure of octahedral voids and how oxygen promotes Nb incorporation is not clear and needs to be investigated further.

Experimental Section

As shown in the chapters above, the influence of impurity elements such as O might play an important role for phase equilibria in Ti-Al based alloys. Therefore, one part of the ADVANCE project is to synthesize alloys with very low impurity contents. For this purpose, high purity Ti (99.995 % HMW Hauner GmbH & Co. KG; 280 wt·ppm

oxygen), Al (99.999 % HMW Hauner GmbH & Co. KG), and Nb (99.95 % HMW Hauner GmbH & Co. KG) are used. Moreover, synthesis methods based on melting alloys in crucibles are omitted. *Tetsui* et al.[31] have shown that the influence of melting time in certain ceramic crucibles on impurity contents is significant. Therefore, a cold crucible levitation melting technique is employed in this project (Figure 5). In this synthesis method, the raw material is levitated and molten in an oscillating electromagnetic field and then cast into a rod-shaped mold.

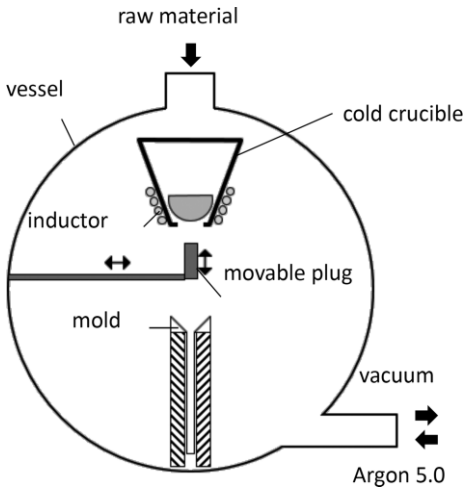

Figure 5. Schematic setup of cold crucible levitation melting device.

Another important factor to keep the impurity content as low as possible is the atmosphere, in which melting is done. Our results (Table 4) show that the condition of the used inert gas plays an important role. Additional drying of the argon gas results in a reduction of the amount of oxygen by a factor of three. The argon in the gas bottles always contains some residual impurities which cannot be removed completely during gas production and filling into the gas bottles.[32] Therefore, additional drying of the gas is required since these impurities provide oxygen for the TiAl alloy during synthesis. Drying can be done in several ways; for example, by drying the argon flow with hot Ti filings[33] before entering the vessel or installing a gas cleaning device (ZPure M™ 3800cc, Chromatography research supplies[34]) to remove the remaining impurities from the gas.

Table 4. Comparison of the oxygen content of alloy Ti-45Al-5Nb synthesized by levitation melting with and without dried argon.

Condition of argon	Oxygen content /ppm
5.0 not dried	770
5.0 dried	250

To minimize contamination during heat treatment, a so-called double crucible technique (Figure 6) described by *Kainuma* et al.[35] is applied. The sample is wrapped into Ta foil and placed in a crucible. This crucible is then placed in a bigger crucible and leftover space is filled with Ti filings. The filings act as getter material and the Ta foil prevents contact between sample and filings. The reaction between Ta and the sample is very sluggish and no Ta was found in any of the samples. The normally used method to encapsulate the samples in fused silica ampoules backfilled with Ti-gettered argon is not applicable as at these temperatures the fused silica ampoules are no longer gas tight[20] and devitrification starts.

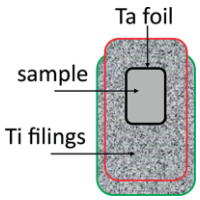

Figure 6. Schematic setup for the employed double crucible technique used for heat treatment at 1300°C.

The samples are quenched in salt water and cut into pieces for different analyses. The oxygen is measured with inert gas fusion (Fusionmaster ONH, NCS Germany) and the overall composition is measured with ICP-AES (Optima 8300, Perkin–Elmer). The phase compositions are measured by EPMA (JEOL JXA-8100 Superprobe) and the phases are identified by means of powder-XRD.

Acknowledgements

This project has received funding from the Clean Sky 2 Joint Undertaking under the European Union's Horizon 2020 research and innovation programme under grant agreement No 820647. Open access funding enabled and organized by Projekt DEAL.

Keywords: Ti-Al alloys; Octahedral voids; Interstitial atoms; Aluminum; Oxygen solubility

References

[1] J. C. Schuster, M. Palm, *J. Phase Equilibria Diffusion* **2006**, *27*, 255–277.
[2] B. P. Bewlay, S. Nag, A. Suzuki, M. J. Weimer, *Mater. High Temperatures* **2016**, *33*, 549–559.
[3] Y. Nishiyama, T. Miyashita, S. Isobe, T. Noda, *Proc. High Temperature Aluminides and Intermetallics* (Eds.: S. H. Wang, C. T. Liu, D. P. Pope and J. O. Stiegler), TMS, Indianapolis, IN, **1990**, 557–584.
[4] H.-L. Lukas, S. G. Fries, B. Sundman, *Computational Thermodynamics: The Calphad Method*, Cambridge University Press, **2007**, 324.
[5] L. A. Bendersky, W. J. Boettinger, B. P. Burton, F. S. Biancaniello, C. B. Shoemaker, *Acta Metallurgica Materialia* **1990**, *38*, 931–943.
[6] H. Clemens, S. Mayer, *Adv. Eng. Mater.* **2013**, *15*, 191–215.
[7] R. M. Waterstrat, Effect of Interstitial Elements on Phase Relationships in the Titanium-Aluminium System, NISTIR 88–3856, National Bureau of Standard and Technology, Gaithersburg, MD, USA; **1988**, 1–53.
[8] H. Nakashima, Y. Kimoto and M. Takeyama, *Proc. Intermetallics 2019* (Eds.: M. Heilmaier, M. Krüger, S. Mayer, M. Palm, F. Stein), Conventus Congress Managment & Marketing GmbH, Jena, Germany, **2019**, 92–93. https://www.intermetallics-conference.de/fileadmin/congress/media/im2019/pdf/Intermetallic_Proceedings_2019.pdf.
[9] Y. Kimoto, H. Nakashima and M. Takeyama, *Proc. Joint EPRI – 123HiMAT International Conference on Advances in High Temperature Materials* (Nagasaki, Japan) ASM International, Materials Park, OH, USA **2019**, pp. 1402–1407.
[10] W. Lefebvre, A. Loiseau, M. Thomas, A. Menand, *Philosophical Magazine A* **2002**, *82*, 2341–2355.
[11] A. Menand, A. Huguet, A. Nérac-Partaix, *Acta Materialia* **1996**, *44*, 4729–4737.

[12] M. X. Zhang, K. C. Hsieh, J. DeKock, Y. A. Chang, *Scripta Metallurgica Materialia* **1992**, *27*, 1361–1366.
[13] H. Clemens, W. Wallgram, S. Kremmer, V. Güther, A. Otto, A. Bartels, *Adv. Eng. Mater.* **2008**, *10*, 707–713.
[14] S. V. Oleynikova, T. T. Nartova, I. I. Kornilov, *Izvestiya Akad. Nauk SSSR, Metally* **1973**, *3*, 184–189.
[15] J. C. Schuster, *Scripta Metallurgica Materialia* **1994**, *30*, 521.
[16] https://www.thermocalcd.com/advance/ page accessed: 24.02.2020.
[17] R. Kainuma, Y. Fujita, H. Mitsui, K. Ishida, *Intermetallics* **2000**, *8*, 855–867.
[18] H. Nakamura, M. Takeyama, L. Wei, Y. Yamabe and M. Kikuchi, *Proc. 3rd Japan International SAMPE Symposium (Chiba)* **1993**, pp. 1353–1358.
[19] S. Xu, Y. Xu, Y. Liang, X. Xu, S. Gao, Y. Wang, J. He, J. Lin, *J. Alloys Compd.* **2017**, *724*, 339–347.
[20] L. Sheng T'sai, T. H. Hogness, *J. Phys. Chem.* **2002**, *36*, 2595–2600.
[21] https://www.heraeus.com/en/hca/fused_silica_quartz_knowledge_base_1/properties_1/properties_hca.html page accessed: 12.02.2020.
[22] S. Becker, A. Rahmel, M. Schorr, M. Schütze, *Oxidation Met.* **1992**, *38*, 425–464.
[23] A. Rahmel, M. Schütze, W. J. Quadakkers, *Mater. Corrosion* **1995**, *46*, 271–285.
[24] Y. Shida, H. Anada, *Mater. Transactions JIM* **1994**, *35*, 623–631.
[25] C. Y. Jones, W. E. Luecke, E. Copland, *Intermetallics* **2006**, *14*, 54–60.
[26] A. Bakulin, A. Latyshev, S. Kulkova, *J. Experimental Theor. Phys.* **2017**, *125*, 138–147.
[27] Y. Wei, H.-B. Zhou, Y. Zhang, G.-H. Lu, H. Xu, *J. Phys.: Condens. Matter* **2011**, *23*, 225504.
[28] W. Zhi, W. Li, H. Gupta, *J. Mater. Sci.* **2007**, *42*, 8139–8143.
[29] M. Dechamps, A. Quivy, G. Baur and P. Lehr, *Scripta Metallurgica* **1977**, *11*, 941–945.
[30] D. Holec, R. K. Reddy, T. Klein, H. Clemens, *J. Appl. Phys.* **2016**, *119*, 205104.
[31] T. Tetsui, T. Kobayashi, T. Ueno, H. Harada, *Intermetallics* **2012**, *31*, 274–281.
[32] https://produkte.linde-gase.de/db_neu/argon_5.0.pdf page accessed: 10.02.2020.
[33] V. T. Witusiewicz, A. A. Bondar, U. Hecht, T. Y. Velikanova, *J. Alloys Compd.* **2009**, *472*, 133–161.
[34] https://www.chromres.com/mwdownloads/download/link/id/87/ page accessed: 02.02.2020.
[35] R. Kainuma, M. Palm, G. Inden, *Intermetallics* **1994**, *2*, 321–332.

Received: February 26, 2020
Published Online: April 8, 2020

